DOI: https://doi.org/10.5114/ceji/209136

The AGO2–ATOX1 axis exacerbates inflammation in a mouse sepsis model

PENG HUANG[1], MEILING HE[2], XIANGYANG MO[1], LIPU DENG[1]

[1]Department of Emergency Medicine, The Affiliated Nanhua Hospital, Hengyang Medical School, University of South China, Hengyang 421002, Hunan, China
[2]Department of Laboratory Medicine, Hengyang First People's Hospital, Hengyang 421002, Hunan, China

Abstract

Introduction: *The study aimed to investigate the mechanism of the Argonaute RISC catalytic component 2 (AGO2)–antioxidant protein 1 (ATOX1) axis in the inflammatory response of sepsis.*

Material and methods: *AGO2 was knocked down by tail vein injection of sh-Ago2 lentivirus, and a sepsis mouse model was established using the cecal ligation and puncture (CLP) method. RAW264.7 cells were transfected with AGO2 or ATOX1 knockdown or overexpression plasmids and treated with lipopolysaccharide (LPS) to construct a cellular sepsis model. Hematoxylin-eosin staining was used to evaluate lung and liver tissue damage in mice. Serum levels of aspartate aminotransferase (AST) and alanine aminotransferase (ALT) were measured using biochemical analysis. ELISA was performed to determine the levels of inflammatory cytokines: tumor necrosis factor α (TNF-α), interleukin (IL)-6, and IL-1β. The expression of AGO2, ATOX1, inducible nitric oxide synthase (iNOS), and arginase 1 (Arg1) was analyzed using RT-qPCR and Western blotting. The effect of AGO2 on ATOX1 mRNA stability was assessed using an actinomycin D assay, and the interaction between AGO2 and ATOX1 was analyzed via RIP-qPCR.*

Results: *AGO2 and ATOX1 were highly expressed in septic mice. In vitro experiments demonstrated that knockdown of AGO2 or ATOX1 suppressed LPS-induced inflammatory responses and macrophage polarization imbalance. AGO2 promoted M1 macrophage polarization and aggravated inflammatory damage by enhancing the stability of ATOX1 mRNA. In vivo experiments further confirmed that AGO2 knockdown significantly alleviated sepsis-induced lung and liver damage, reduced the inflammatory response, and inhibited ATOX1 expression.*

Conclusions: *AGO2 binds to ATOX1 mRNA, promoting ATOX1 expression, inducing macrophage polarization imbalance, and exacerbating sepsis-induced inflammatory responses.*

Key words: *sepsis, AGO2, ATOX1, macrophage polarization, inflammatory response.*

(Cent Eur J Immunol 2026; 51: 1-15)

Introduction

Sepsis is a systemic inflammatory response syndrome caused by pathogenic microbial infections, characterized by an excessive host response to infection [1]. This abnormal response can trigger severe systemic inflammation through the bloodstream, leading to microcirculatory dysfunction, tissue hypoxia, multiple organ injury, and ultimately organ failure [2]. Sepsis presents with diverse clinical manifestations, often accompanied by pathological phenomena such as increased microvascular permeability, fluid extravasation, and excessive release of inflammatory cytokines. These changes exacerbate the severity of the disease and may result in mortality [3, 4]. Globally, sepsis accounts for approximately 11 million deaths annually, representing one-fifth of all mortality cases [5, 6]. Despite advances in sepsis treatment in recent years, its complex pathogenesis and therapeutic challenges remain a significant global medical research priority. Macrophages, key components of the innate immune system, play a central role in pathogen recognition and clearance as well as in regulating immune responses [7]. Macrophages can polarize into pro-inflammatory M1 and anti-inflammatory M2 phenotypes. M1 macrophages assist in pathogen clearance by secreting pro-inflammatory cytokines such as tumor necrosis factor α (TNF-α) and interleukin (IL)-6, but excessive activation may lead to uncontrolled inflammation and aggravated tissue damage. In contrast, M2 macrophages secrete anti-inflammatory cytokines such as IL-10 and transforming growth factor β (TGF-β) to regulate inflammation and promote tissue repair [8]. Studies have shown that macrophage polarization is a critical factor in determining the stage of inflammation. Macrophage polarization, pyroptosis, and phagocytosis con-

Correspondence: Lipu Deng, Department of Emergency Medicine, The Affiliated Nanhua Hospital, Hengyang Medical School, University of South China, No. 336 Dongfeng South Road, Zhuhui District, Hengyang, Hunan Province, China, e-mail: m17773437262@163.com

Submitted: 10.04.2025, Accepted: 08.08.2025

tribute to the inflammatory processes in sepsis-induced acute lung injury and dynamically switch between pro-inflammatory M1 and anti-inflammatory M2 phenotypes in response to microenvironmental signals [9, 10]. Therefore, macrophage polarization plays a pivotal role in the pathogenesis of sepsis, and targeting the regulation of macrophage polarization to balance the M1/M2 ratio is a promising therapeutic strategy for sepsis.

In recent years, the Argonaute protein family, particularly Argonaute RISC catalytic component 2 (AGO2), has garnered significant attention due to its central role in RNA interference and post-transcriptional regulation [11]. AGO2 can influence gene expression and cellular functions by regulating mRNA [12]. Studies have demonstrated that AGO2 modulates the release of inflammatory cytokines through miRNA network regulation [13]. In the context of sepsis, changes in AGO2 expression are closely associated with cytokine release and immune dysfunction [14]. Furthermore, dysregulation of AGO2 can result in miRNA processing defects and aberrant expression of pro-inflammatory genes, exacerbating the inflammatory response in sepsis [15]. Antioxidant protein 1 (ATOX1), a metallochaperone protein, plays a key role in intracellular copper transport and redox homeostasis, while also serving as a critical regulator of inflammatory processes [16]. ATOX1 promotes the production of reactive oxygen species and upregulates pro-inflammatory gene expression through copper-dependent mechanisms [17, 18]. Moreover, ATOX1 activates the NLRP3 inflammasome pathway to promote M1 macrophage polarization and amplify the inflammatory response. Silencing ATOX1 has been shown to significantly attenuate inflammation, inhibit M1 polarization, and mitigate tissue damage [19]. While the involvement of ATOX1 in inflammation and macrophage polarization has been increasingly recognized, it remains unclear whether AGO2 exerts its pro-inflammatory effects in sepsis by regulating ATOX1. This study systematically investigated the mechanism of the AGO2–ATOX1 axis in sepsis-induced inflammatory responses using a cecal ligation and puncture (CLP) mouse model *in vivo*, and a lipopolysaccharide (LPS)-stimulated RAW264.7 macrophage model with AGO2 or ATOX1 knockdown or overexpression *in vitro*. Our results highlight the pivotal role of this axis in modulating macrophage polarization and the inflammatory response. These findings provide a theoretical basis for fundamental research and clinical treatment of sepsis and offer valuable insights for the development of novel therapeutic strategies and targets.

Material and methods

Experimental animals

The male ICR mice (8 weeks old, weighing 38 ±3 g) were purchased from Hunan SJA Laboratory Animal Co., Ltd (Changsha, China). All mice were housed in the animal center laboratory under controlled environmental conditions: temperature 24 ±1°C, humidity 60 ±5%, and a 12-hour light/dark cycle. Standard chow and water were provided *ad libitum*. All animal procedures were approved by the Animal Ethics Committee and conducted in accordance with the 3Rs principle (replacement, reduction, and refinement).

Bioinformatics analysis

The sepsis dataset GSE137342 was downloaded from the Gene Expression Omnibus database. The raw count matrix of GSE137342 was analyzed using the DESeq2 package (v1.38.3) in R (v4.3.1). Differential expression analysis was performed using the Wald test based on a negative binomial generalized linear model, and p values were adjusted for multiple testing using the Benjamini-Hochberg method. Differentially expressed genes (DEGs) were identified using the criteria P adj. < 0.01 and logFC > 2. RNA-binding protein (RBP) genes related to RNA stability were obtained from the CLIPdb database (http://111.198.139.65/RBP.html). DEGs were intersected with RBP genes to identify core RBPs. Subsequently, downstream targets of the core RBP were predicted using CLIPdb and further intersected with DEGs. The intersected genes were ranked in ascending order based on the adjusted p values (P adj.) using Excel software, and the most significantly altered key gene in sepsis was identified.

Establishment of a sepsis mouse model

A total of 32 mice were randomly divided into four groups ($n = 32$): sham, model, sh-NC, and sh-Ago2, with 8 mice in each group. The sepsis mouse model was established using CLP surgery. Mice were fasted for 12 hours prior to surgery and anesthetized with isoflurane (792632, Sigma-Aldrich, Shanghai, China). In the sham-operated group (sham), an abdominal incision was made to expose the distal cecum and mesentery without further intervention, followed by abdominal closure. In the model group (model), CLP surgery was performed. Specifically, after routine disinfection, a 2 cm midline incision was made in the abdomen to expose the cecum. The distal cecum was separated from the mesentery while avoiding vascular injury. The cecum was ligated three-fourths of the way from its distal end using sterile 4-0 sutures. A sterile 7-gauge needle was used to puncture the cecal wall between the ligation site and the cecal tip. After perforation, the abdominal cavity was closed layer by layer [20]. The model group was subdivided into three subgroups: model (untreated), sh-Ago2, and sh-NC. In the sh-Ago2 and sh-NC groups, shRNA AAV9 viral vectors targeting AGO2 (sh-Ago2) and control shRNA (sh-NC) were injected *via* the tail vein one week before the CLP procedure (shRNA lentiviruses were constructed by Shanghai GeneChem Co., Ltd.). At 48 hours after CLP, blood serum was collected, and mice were euthanized with an overdose of sodium pentobarbital (100 mg/kg). Lung and liver tissues were then harvested. Collected samples were used for subsequent experimental analyses.

Construction of a sepsis cell model

RAW264.7 cells (CL-0190, Procell, Wuhan, China) were cultured in Dulbecco's modified Eagle medium (12491015, Gibco, Shanghai, China) supplemented with 10% fetal bovine serum (F0193, Sigma, Shanghai, China), 100 mg/ml streptomycin, and 100 µg/ml penicillin (15070063, Gibco, Shanghai, China). When cell confluence reached 70-80%, plasmids including sh-NC, sh-Ago2, sh-Atox1, oe-NC, and oe-Atox1 (synthesized by GeneChem Co., Ltd., Shanghai, China) were transfected into RAW264.7 cells using Lipofectamine 3000 (L3000001, Thermo Fisher, Shanghai, China). After 48 hours of transfection, AGO2 and ATOX1 expression levels were assessed using reverse transcription quantitative polymerase chain reaction (RT-qPCR) to confirm transfection efficiency. Subsequently, cells were stimulated with 1 µg/ml LPS for 48 hours to construct the sepsis cell model [20]. Cells were divided into 8 groups based on treatments: phosphate buffer saline (PBS; control), LPS, LPS + sh-NC, LPS + sh-Ago2, LPS + sh-Atox1, sh-NC + oe-NC, sh-Ago2 + oe-NC, and sh-Ago2 + oe-Atox1. After 48 hours, cells and supernatants were collected for subsequent analyses.

Hematoxylin and eosin staining

Mouse lung and liver tissues were fixed in 4% paraformaldehyde solution (441244, Sigma, Shanghai, China), embedded in paraffin, and sectioned. The paraffin sections were cleared with xylene (534056, Sigma), followed by dehydration through a graded ethanol series and immersion in distilled water for 2 minutes. The sections were stained with ematoxylin and eosin (HE) staining solutions (G1120, Solarbio, Shanghai, China) for 3 minutes and 1 minute, respectively. After staining, the sections were dehydrated with graded ethanol and cleared with xylene. Finally, the sections were mounted and observed under an optical microscope (XDS-30, BINGYU, Shanghai, China).

Biochemical analysis for aspartate aminotransferase and alanine aminotransferase levels

Serum aspartate aminotransferase (AST) levels were measured using the AST Assay Kit (MAK467, Sigma). Detection reagents were prepared according to the manufacturer's instructions. A 96-well plate was loaded with 20 µl of serum (with NADH standard and 20 µl of H_2O serving as calibration and blank controls, respectively) and 200 µl of detection reagent. After mixing, the plate was incubated at 37°C. Optical density (OD) values at 340 nm were recorded at the 5th and 10th minutes using a microplate reader (168-1130, Bio-Rad, USA).

Serum alanine aminotransferase (ALT) levels were measured using the ALT Activity Assay Kit (MAK052, Sigma). Briefly, 20 µl of serum was added to a 96-well plate, and reaction solutions were prepared according to the kit instructions. Subsequently, 100 µl of reaction solution was added to each sample, positive control, and standard well. After mixing, the plate was left to stand for 2 minutes. OD values were measured at 570 nm at 5-minute intervals until the sample well OD values exceeded the standard well values.

Enzyme-linked immunosorbent assay for TNF-α, IL-6, and IL-1β levels

Enzyme-linked immunosorbent assay (ELISA) kits specific for mouse TNF-α (88-7324-88, Thermo Fisher, Shanghai, China), IL-6 (88-7064-88, Thermo Fisher, Shanghai, China), and IL-1β (88-7013-22, Thermo Fisher, Shanghai, China) were used to measure the levels of these cytokines in serum or cell culture supernatants. In brief, 100 µl of serum or standard solution was added to ELISA plates pretreated with capture antibody buffer and ELISA/ELISPOT dilution buffer (1×). Plates were incubated at room temperature for 2 hours. After washing, 100 µl of detection antibody was added, followed by incubation at room temperature for 1 hour. After another washing step, 100 µl of Streptavidin-HRP was added, and the plates were sealed and incubated at room temperature for 30 minutes. Following a final wash, 100 µl of stop solution was added, and OD values were recorded at 450 nm using a microplate reader.

Western blot analysis of protein expression

Proteins from tissues and cells were extracted using radioimmunoprecipitation assay lysis buffer (R0278, Sigma, Shanghai, China), and protein concentration was measured using the BCA method (A55861, Thermo Fisher, Shanghai, China). After separating the proteins by sodium dodecyl sulfate-polyacrylamide gel electrophoresis, they were transferred to polyvinylidene difluoride membranes and blocked with 5% non-fat milk for 1 hour. The membranes were then incubated overnight at 4°C with primary antibodies against AGO2 (1 : 1000, ab186733, Abcam, Shanghai, China), ATOX1 (1 : 500, 31090-1-AP, Proteintech, Wuhan, China), inducible nitric oxide synthase (iNOS; 1 : 1000, ab178945, Abcam, Shanghai, China), arginase 1 (Arg1; 1 : 1000; ab315110, Abcam), and β-actin (1 : 1000; ab8227, Abcam). After washing, the membranes were incubated with HRP-conjugated goat anti-rabbit immunoglobulin G (IgG; 1 : 2000; ab205718, Abcam) for 1 hour at room temperature. The protein bands were visualized using enhanced chemiluminescent reagent (MA0186, Meilunbio, Liaoning, China). Relative protein expression levels were quantified using ImageJ software (V1.8.0.112, NIH, Madison, WI, USA), with β-actin as the internal control. Western blot analysis was performed across all experimental groups to comprehensively evaluate the expression levels of various relevant proteins under different treatment conditions.

RT-qPCR for gene expression

Total RNA from RAW264.7 cells was extracted using TRIzol reagent (15596026CN, Thermo Fisher, Shanghai, China), and cDNA was synthesized from RNA using the Hifair AdvanceFast 1st Strand cDNA Synthesis SuperMix for qPCR kit (11156ES10, Yesen, Shanghai, China). Gene amplification was performed using the Hieff UNICON Universal Blue qPCR SYBR Green Master Mix kit (11184ES08, Yesen, Shanghai, China) on a LightCycler 480 real-time PCR instrument (Roche, Basel, Switzerland). The PCR conditions were as follows: 95°C for 30 s; 95°C for 3 s; 60°C for 20 s; 40 cycles, with a default dissociation curve setting. Relative gene expression was calculated using the $2^{-\Delta\Delta CT}$ method with β-actin as the internal reference. The primers used are listed in Table 1. RT-qPCR was performed in LPS-induced RAW264.7 cells, including the AGO2-silenced groups (sh-NC, sh-Ago2-1, sh-Ago2-2) and the ATOX1-silenced groups (sh-NC, sh-Atox1-1, sh-Atox1-2), to assess gene expression.

RNA half-life assay

To assess the stability of ATOX1 mRNA under AGO2 knockdown, cells were treated with the transcription inhibitor actinomycin D (2 mg/ml; SBR00013, Sigma, Shanghai, China). RNA was extracted from cells at 0, 2, 4, and 6 hours after treatment and analyzed *via* RT-qPCR. ATOX1 mRNA levels were normalized to β-actin, and the relative expression at each time point was calculated.

RNA immunoprecipitation (RIP-qPCR) assay

RIP-qPCR analysis was performed using the Smart-RIP RIP Kit (RIP-1001, Engibody, Dover, America). Cell lysates were incubated overnight at 4°C with magnetic beads conjugated to either AGO2 or IgG antibodies. After magnetic separation and removal of the supernatant, beads were washed and resuspended in lysis buffer to collect RNA-protein complexes. RNA was extracted according to the kit instructions, and ATOX1 mRNA enrichment levels were quantified *via* RT-qPCR.

Table 1. Primer sequences

Gene	Primer sequence (5’-3’)
AGO2	F: CACCTGAAGAACACATACGCTGG
	R: TGTGTCTCCCACACGCTTGACT
ATOX1	F: ATGCCGAAGCACGAGTTCTC
	R: ATGCAGACCTTCTTGTTGGGC
β-actin	F: GGCTGTATTCCCCTCCATCG
	R: CCAGTTGGTAACAATGCCATGT

Statistical analysis

Statistical analyses were performed using GraphPad Prism 9. Quantitative data were expressed as mean ± standard error of the mean (SEM). A *t*-test was used for comparisons between two groups, while one-way or two-way analysis of variance (ANOVA) followed by Tukey’s post hoc test with adjustment for multiple comparisons was applied for comparisons among three or more groups. In the case of nonparametric data, the Kruskal-Wallis test followed by Dunn’s multiple comparisons test with Bonferroni correction was used. A value of $p < 0.05$ was considered statistically significant.

Results and analysis

AGO2 mediates macrophage polarization imbalance to exacerbate the sepsis-induced inflammatory response

A total of 194 DEGs were identified from the GSE137342 dataset (Fig. 1A). These DEGs were intersected with 71 RBP genes associated with RNA stability, revealing AGO2 (Fig. 1B), which was significantly upregulated in sepsis (Fig. 1C). To assess the role of AGO2 in the inflammatory response during sepsis, we established a sepsis mouse model. The results showed that, compared to the sham group, the model group exhibited damaged lung tissue with thickened alveolar septa. Liver tissue showed cell necrosis and increased infiltration of inflammatory cells (Fig. 1D), along with significantly elevated levels of the serum liver injury markers AST and ALT (Fig. 1E), indicating organ damage caused by sepsis. Additionally, levels of the serum pro-inflammatory cytokines TNF-α, IL-6, and IL-1β were significantly elevated, further exacerbating the inflammatory response (Fig. 1F). These findings confirmed the successful establishment of the sepsis mouse model.

Further analysis revealed that in the model group, the expression of iNOS (a marker for M1 polarization) was significantly upregulated, while Arg1 (a marker for M2 polarization) was downregulated. Concurrently, AGO2 expression was significantly elevated in the lung and liver tissues of septic mice, consistent with bioinformatics analysis results (Fig. 1G, H). These findings suggest that AGO2 may contribute to the progression of sepsis by influencing macrophage polarization imbalance.

Silencing AGO2 regulates macrophage polarization and inhibits the LPS-induced inflammatory response

To investigate whether AGO2 mediates the LPS-induced inflammatory response through the regulation of

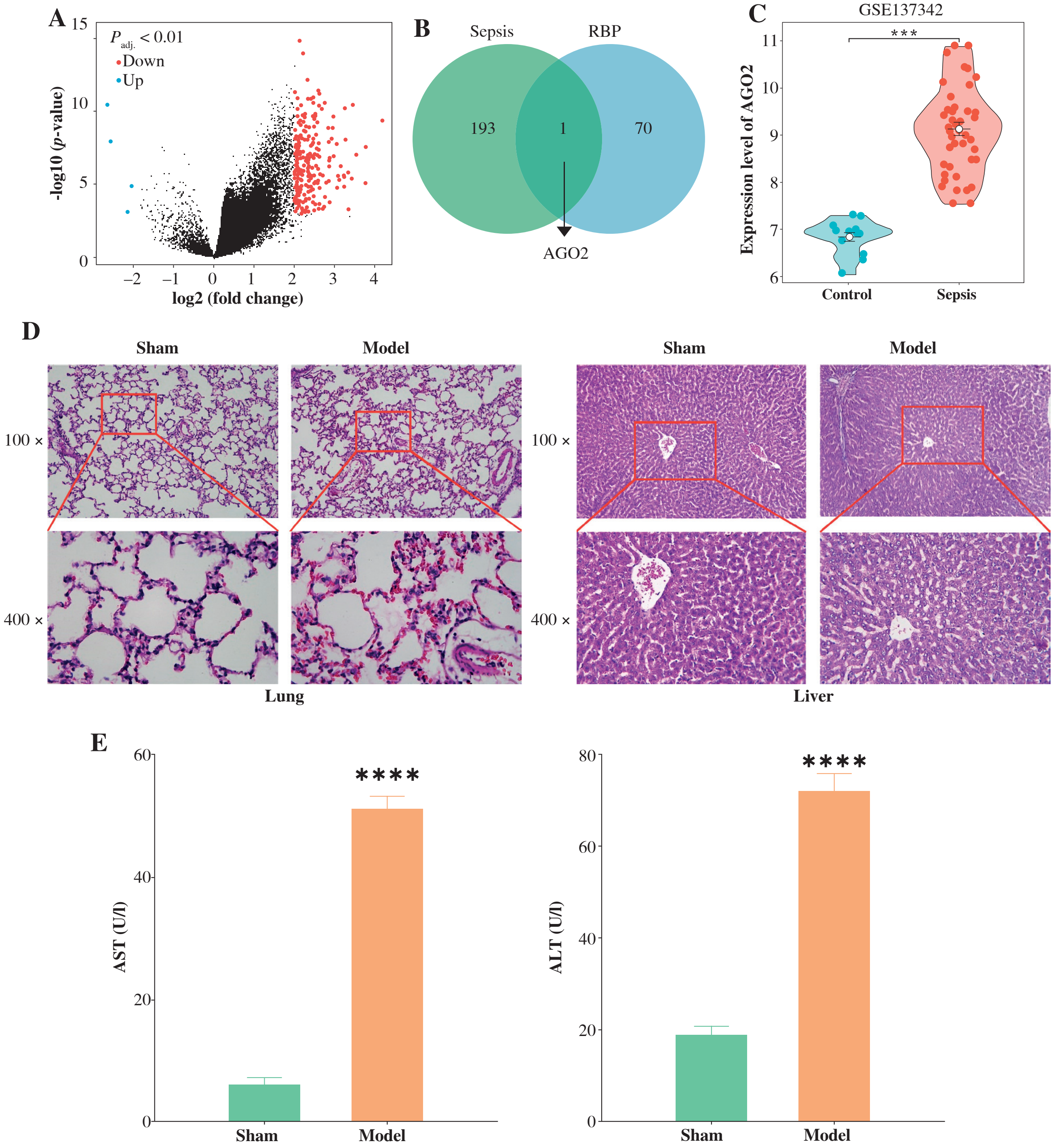

Fig. 1. AGO2 mediates macrophage polarization imbalance to exacerbate sepsis-induced inflammatory response. **A**) Volcano plot of differential analysis from the GSE137342 dataset; **B**) Intersection of DEGs in sepsis with RBP genes; **C**) Expression of AGO2 in the sepsis dataset GSE137342; **D**) HE staining of lung and liver tissue showing damage in mice (100×); **E**) Biochemical analysis of AST and ALT levels in serum. $N = 8$, ****$p < 0.0001$

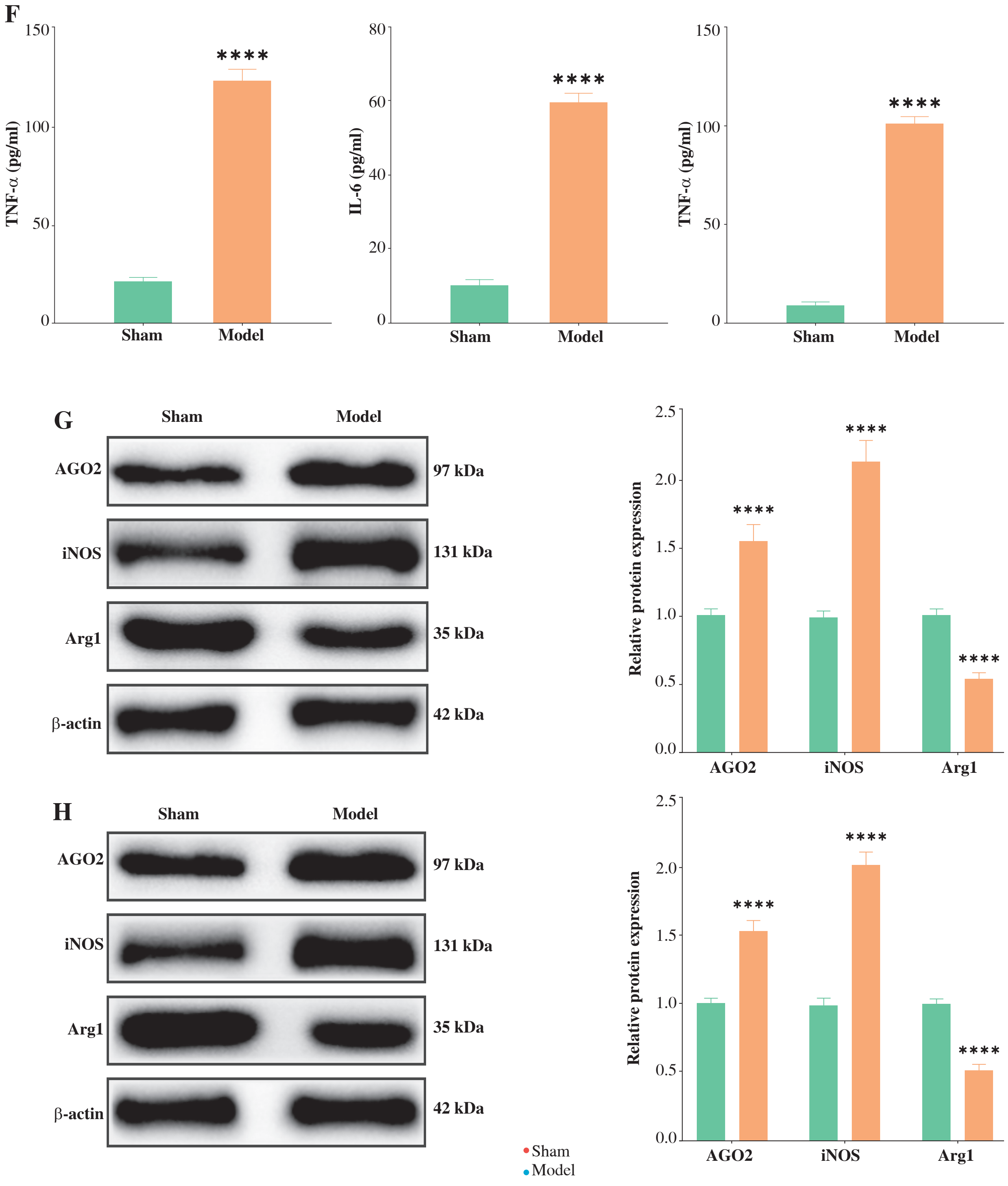

Fig. 1. Cont. **F**) ELISA detection of serum TNF-α, IL-6, and IL-1β levels; **G**, **H**) Western blot analysis of AGO2, iNOS, and Arg1 expression in mouse lung (**G**) and liver tissues (**H**). $N = 8$, $^{****}p < 0.0001$

macrophage polarization, we constructed a sepsis cell model with sh-Ago2. RT-qPCR was used to verify the silencing efficiency of AGO2, and the sh-Ago2-1 construct with the highest silencing efficiency was selected for further experiments (Fig. 2A). The results showed that, compared to the PBS group, LPS stimulation significantly upregulated the expression of AGO2 and iNOS, while downregulating Arg1 expression.

However, silencing AGO2 reversed these gene expression changes, promoting macrophage polarization towards the M2 phenotype (Fig. 2B, C). Furthermore, LPS treatment significantly increased the levels of TNF-α and IL-6

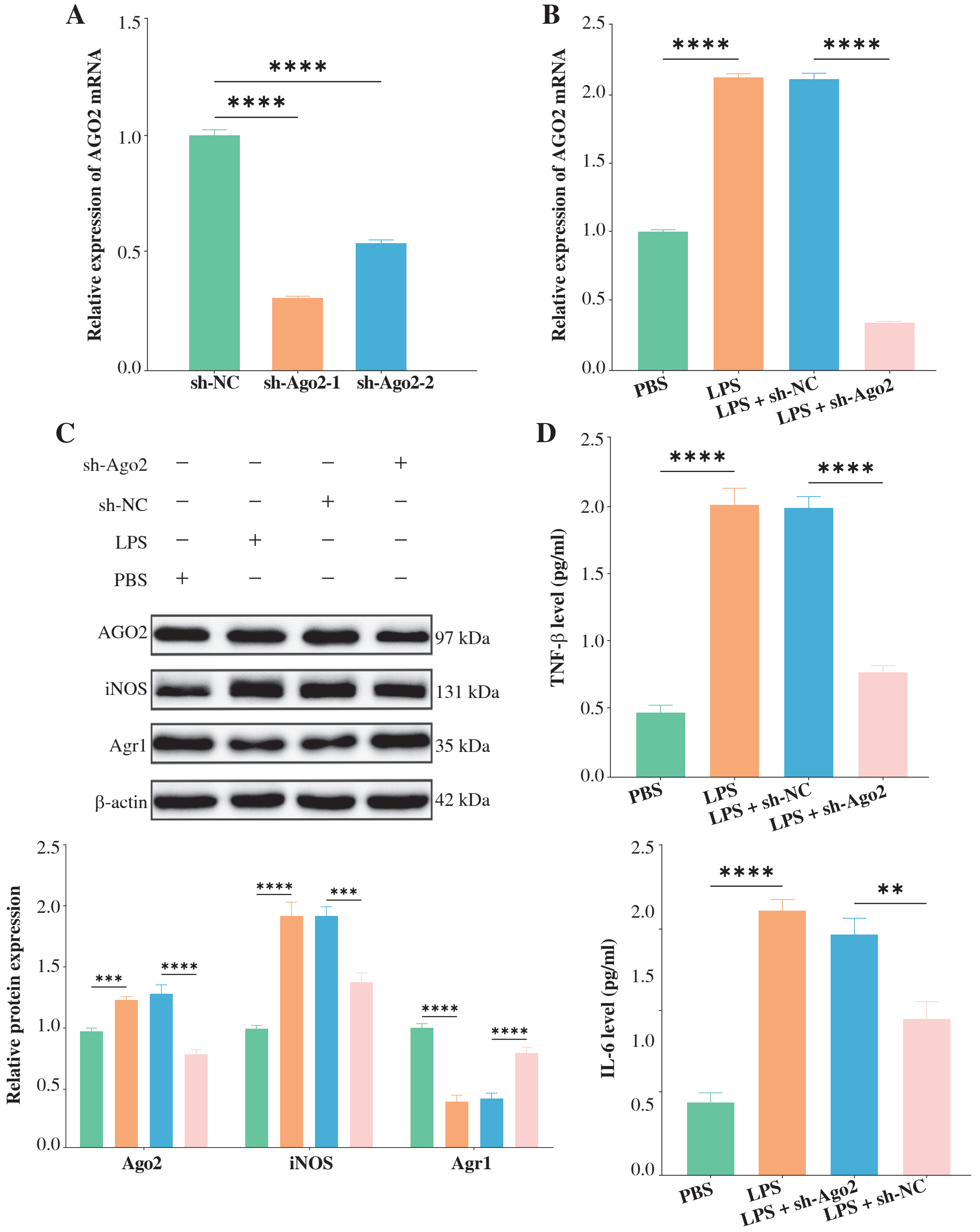

Fig. 2. Silencing AGO2 regulates macrophage polarization and inhibits the LPS-induced inflammatory response. **A**) RT-qPCR to verify the silencing efficiency of sh-Ago2; **B**) RT-qPCR detection of AGO2 expression in cells; **C**) Western blot analysis of AGO2, iNOS, and Arg1 expression in cells; **D**) ELISA detection of TNF-α and IL-6 levels in cell culture supernatants. Cell experiments were performed in triplicate. **$p < 0.01$, ***$p < 0.001$, ****$p < 0.0001$

in the cell culture supernatant, while AGO2 knockdown effectively reduced these inflammatory cytokine levels (Fig. 2D).

These findings suggest that downregulation of AGO2 expression can correct macrophage polarization imbalance, thereby inhibiting the LPS-induced inflammatory response.

Silencing ATOX1 regulates macrophage polarization and inhibits the LPS-induced inflammatory response

To further explore the specific regulatory mechanism of AGO2, we intersected 15,487 downstream targets of AGO2 predicted from the CLIPdb database with the sep-

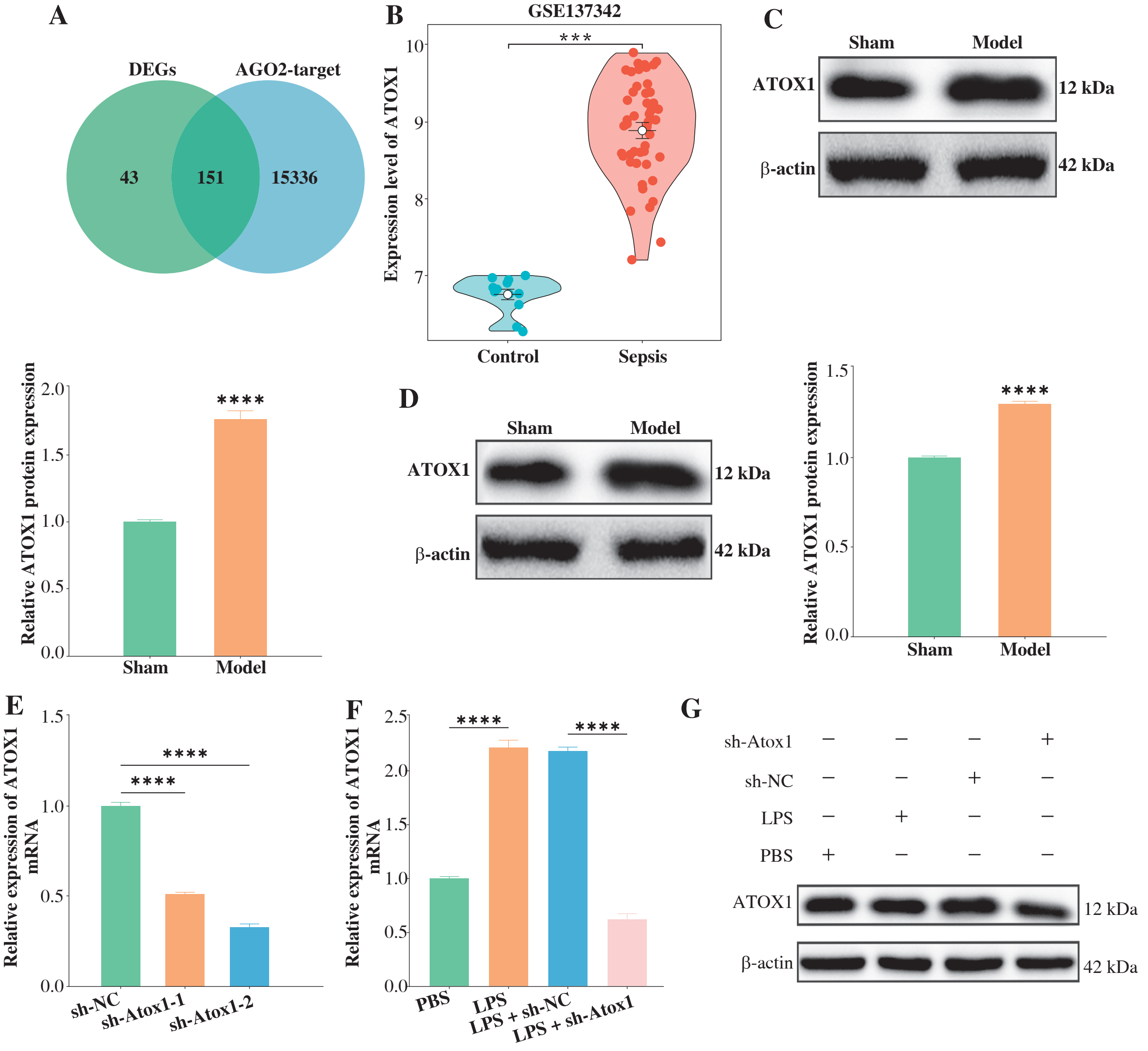

Fig. 3. Silencing ATOX1 regulates macrophage polarization and inhibits the LPS-induced inflammatory response. **A**) Intersection of sepsis DEGs and AGO2 downstream targets; **B**) Expression of ATOX1 in the sepsis dataset GSE137342; **C**, **D**) Western blot analysis of ATOX1 expression in lung (**C**) and liver tissues (**D**) from septic mice ($N = 8$); **E**) RT-qPCR detection of sh-Atox1 silencing efficiency; **F**, **G**) RT-qPCR (**F**) and Western blot (**G**) detection of ATOX1 expression in cells; **H**) Western blot detection of iNOS and Arg1 expression in cells; **I**) ELISA detection of TNF-α and IL-6 levels in cell culture supernatant. Cell experiments were performed in triplicate. $^{***}p < 0.001$, $^{****}p < 0.0001$

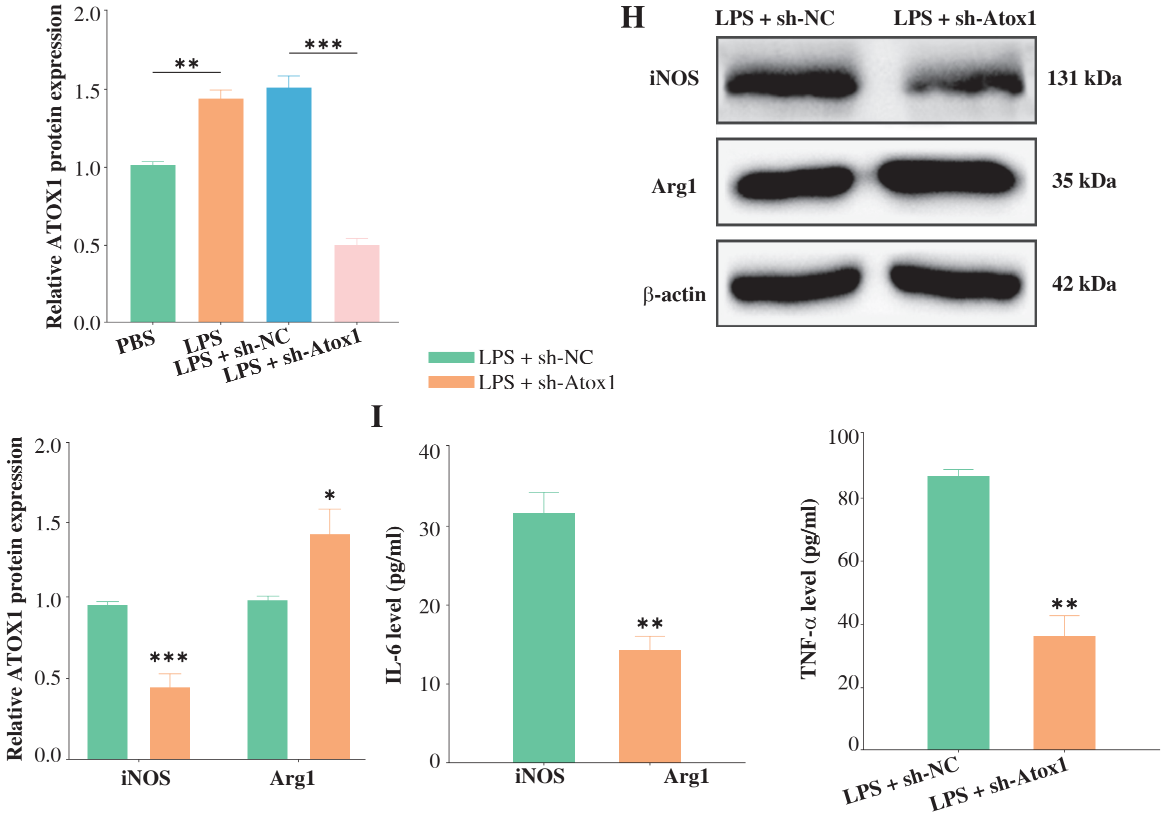

Fig. 3. Cont. **G**) RT-qPCR (**F**) and Western blot (**G**) detection of ATOX1 expression in cells; **H**) Western blot detection of iNOS and Arg1 expression in cells; **I**) ELISA detection of IL-6 and TNF-α levels in cell culture supernatant. Cell experiments were performed in triplicate. $^{*}p < 0.05$, $^{**}p < 0.01$, $^{***}p < 0.001$, $^{****}p < 0.0001$

sis DEGs, resulting in the identification of 151 common genes (Fig. 3A). We then selected the top 10 significantly differentially expressed intersecting genes with the lowest *P* adj. values: MYL6, UBASH3B, TPD52L2, GSTO1, HIST1H2BK, NAPRT, ATOX1, TPST2, MRPL36, and TMEM256. Among these, ATOX1 was highly expressed in sepsis (Fig. 3B). As expected, ATOX1 expression was significantly upregulated in the lungs and livers of model group mice, further supporting our bioinformatics analysis results (Fig. 3C, D).

Subsequently, we constructed the sh-Atox1 sepsis cell model to investigate whether ATOX1 influences the inflammatory response through the regulation of macrophage polarization. RT-qPCR identified the sh-Atox1-2 construct with the highest silencing efficiency for subsequent experiments (Fig. 3E). The results showed that ATOX1 expression was significantly elevated in LPS-treated cells compared to the PBS group. Silencing ATOX1 dramatically reduced its expression levels (Fig. 3F, G). At the same time, silencing ATOX1 significantly inhibited iNOS expression and promoted Arg1 expression (Fig. 3H). Moreover, silencing ATOX1 also significantly reduced TNF-α and IL-6 levels in the cell culture supernatant, thus alleviating the inflammatory response (Fig. 3I). These findings indicate that ATOX1 plays an important role in the LPS-induced inflammatory response by mediating macrophage polarization imbalance.

AGO2 enhances ATOX1 mRNA stability

To elucidate the regulatory mechanism between AGO2 and ATOX1, we conducted several experiments. The results showed that, compared to the LPS + sh-NC group, the expression of ATOX1 was significantly downregulated in the LPS + sh-Ago2 group (Fig. 4A). We then treated the cells with actinomycin D and found that silencing AGO2 significantly shortened the half-life of ATOX1 mRNA, reducing its stability (Fig. 4B). Additionally, we performed RIP-qPCR experiments to further examine the interaction between AGO2 and ATOX1 mRNA. The results indicated that AGO2 directly binds to ATOX1 mRNA (Fig. 4C). This finding not only confirms the direct interaction between AGO2 and ATOX1 but also reveals the molecular mechanism by which AGO2 enhances ATOX1 mRNA stability to upregulate its expression.

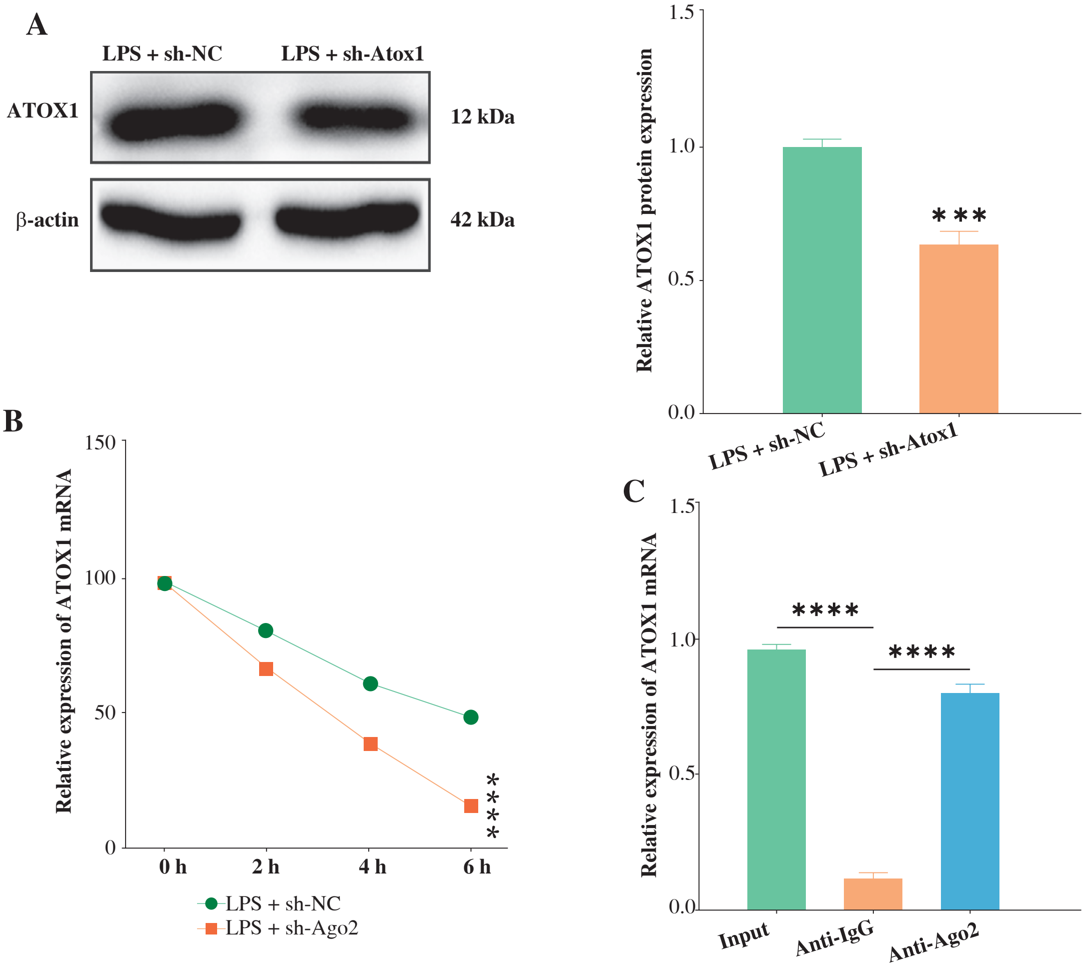

Fig. 4. AGO2 enhances ATOX1 mRNA stability. **A**) Western blot analysis of ATOX1 expression in cells; **B**) Actinomycin D treatment to measure the half-life of ATOX1 mRNA; **C**) RIP-qPCR analysis of AGO2 binding to ATOX1 mRNA. Cell experiments were performed in triplicate. ***$p < 0.001$, ****$p < 0.0001$

AGO2 promotes macrophage polarization imbalance and aggravates the inflammatory response by enhancing ATOX1 mRNA stability

We further assessed whether AGO2 regulates macrophage polarization and inflammation through ATOX1. To this end, we overexpressed ATOX1 in the AGO2 knockdown septic cell model. The results showed that AGO2 knockdown significantly inhibited the expression of ATOX1 and iNOS, while upregulating the expression of Arg1. However, overexpression of ATOX1 restored the levels of ATOX1, iNOS, and Arg1, without significantly affecting AGO2 expression (Fig. 5A). Additionally, AGO2 silencing reduced levels of the inflammatory factors TNF-α and IL-6, and ATOX1 overexpression counteracted the inhibitory effect of AGO2 silencing (Fig. 5B). These results suggest that AGO2 enhances ATOX1 mRNA stability and upregulates ATOX1 expression, promoting M1 macrophage polarization and aggravating the inflammatory response.

AGO2 aggravates the sepsis-induced inflammatory response by mediating macrophage polarization imbalance through ATOX1

To further validate the impact of the AGO2–ATOX1 axis on macrophage polarization and inflammation in the septic mouse model, we administered sh-Ago2 lentivirus *via* tail vein injection. The experimental results showed that, compared to the sh-NC group, the sh-Ago2 group exhibited reduced lung and liver tissue damage, decreased inflammatory cell infiltration, and significantly lower serum levels of AST and ALT (Fig. 6A, B), indicating that silencing AGO2 alleviates organ damage caused by sepsis. More-

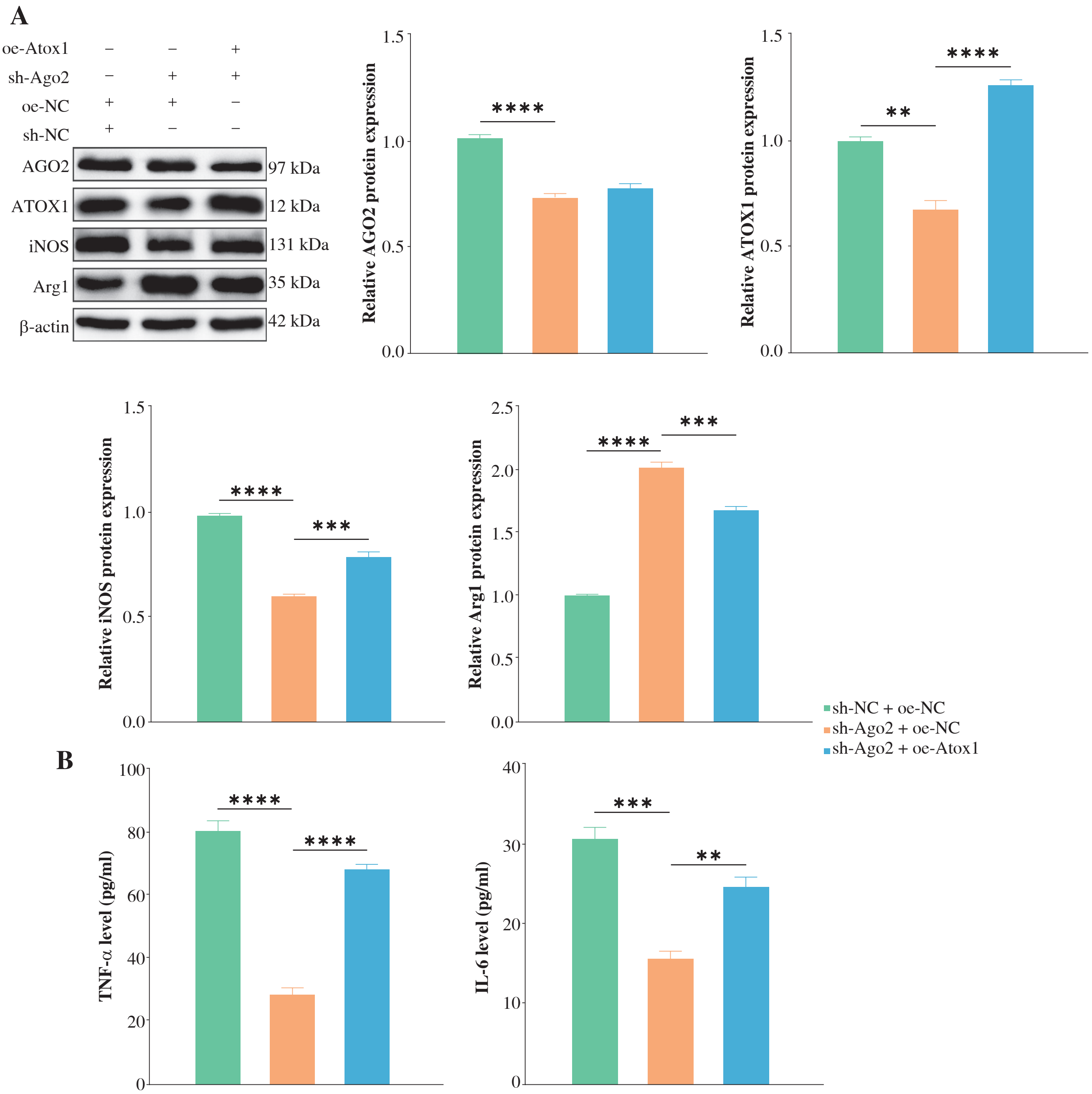

Fig. 5. AGO2 promotes macrophage polarization imbalance and aggravates the inflammatory response by enhancing ATOX1 mRNA stability. **A**) Western blot analysis of AGO2, ATOX1, iNOS, and Arg1 expression in cells; **B**) ELISA measurement of TNF-α and IL-6 levels in cell culture supernatant. Cell experiments were performed in triplicate. $^{**}p < 0.01$, $^{***}p < 0.001$, $^{****}p < 0.0001$

over, AGO2 knockdown significantly reduced the levels of TNF-α, IL-6, and IL-1β in the serum, effectively inhibiting the inflammatory response in septic mice (Fig. 6C). Further analysis revealed that the expression of iNOS, AGO2, and ATOX1 in the tissues of the sh-Ago2 group was significantly reduced, while the expression of Arg1 was significantly upregulated, suggesting a shift of macrophages toward M2 polarization (Fig. 6D, E). Taken together, AGO2 upregulates ATOX1 expression, promotes M1 macrophage polarization, and mediates polarization imbalance, thereby exacerbating the inflammatory response in septic mice.

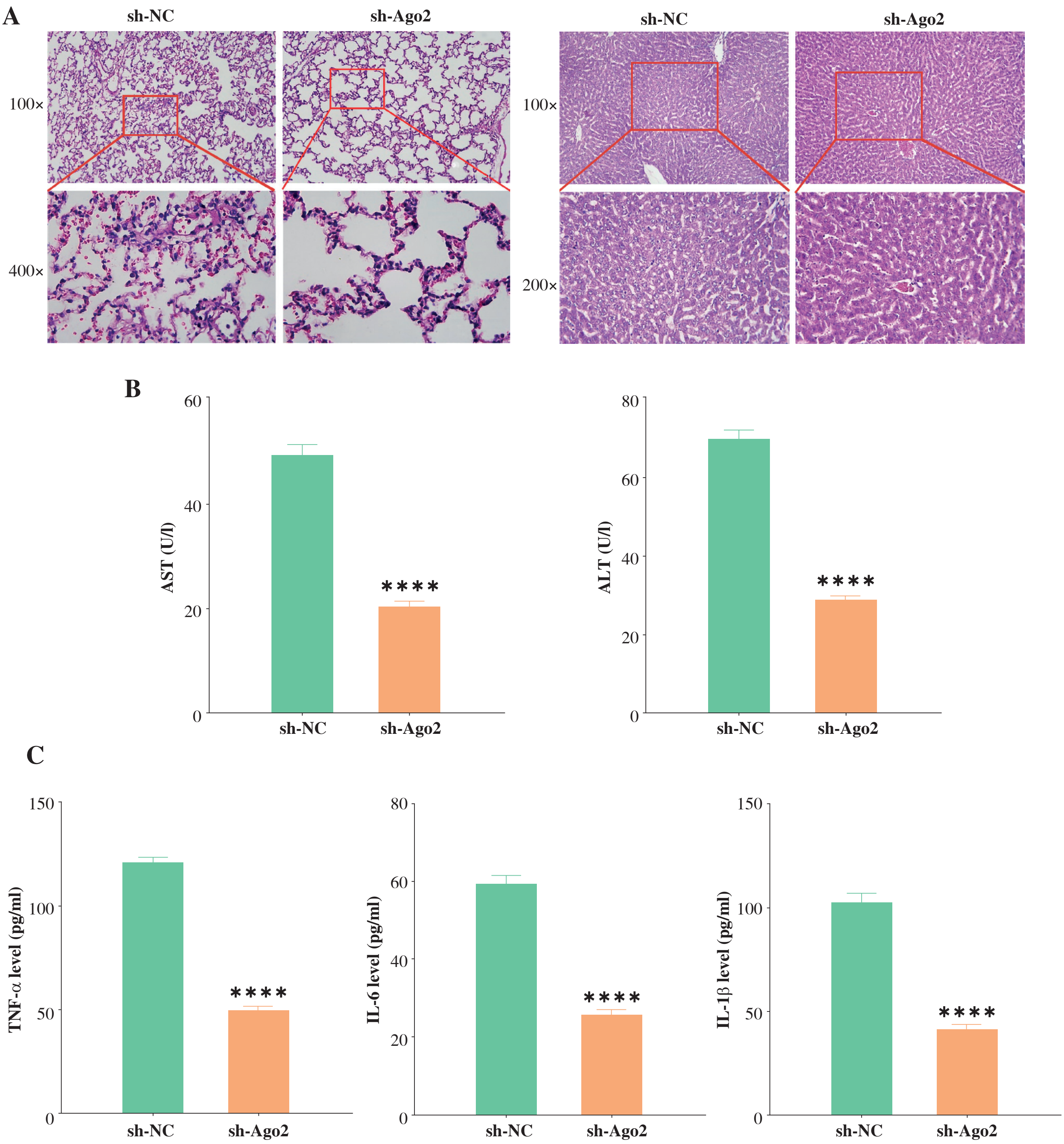

Fig. 6. AGO2 aggravates the sepsis-induced inflammatory response by mediating macrophage polarization imbalance through ATOX1. **A**) HE staining to observe pathological changes in mouse lung and liver tissues (100×); **B**) Biochemical analysis of serum AST and ALT levels; **C**) ELISA detection of serum TNF-α, IL-6, and IL-1β levels. $N = 8$, $^{****}p < 0.0001$

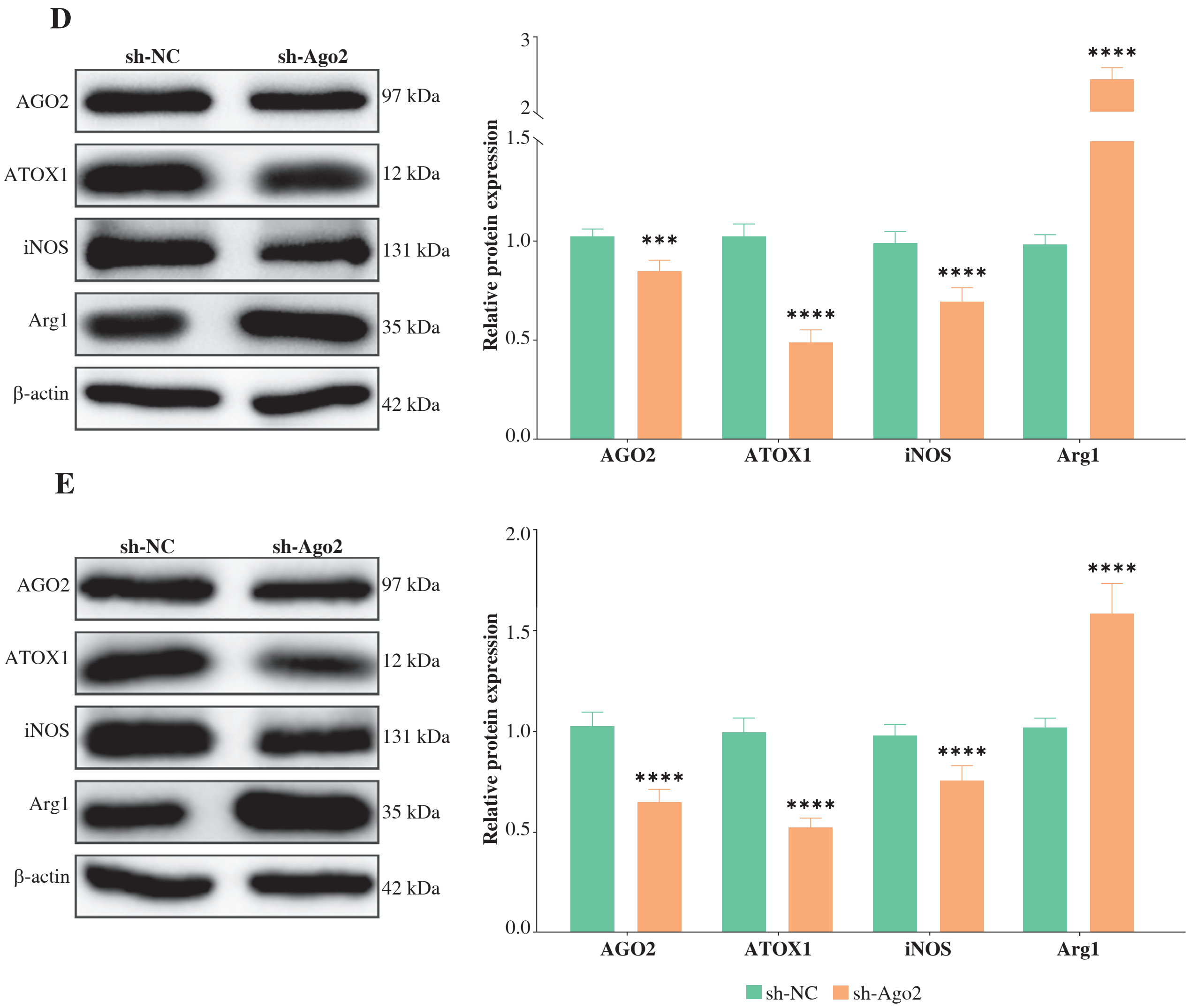

Fig. 6. Cont. AGO2 aggravates the sepsis-induced inflammatory response by mediating macrophage polarization imbalance through ATOX1. **D**, **E**) Western blot analysis of iNOS, Arg1, AGO2, and ATOX1 expression in mouse lung (**D**) and liver tissues (**E**). $N = 8$, $***p < 0.001$, $****p < 0.0001$

Discussion

Sepsis is a dysfunctional disease caused by dysregulated host responses to infection, and it is one of the leading causes of high morbidity and mortality in postoperative patients. During the early stages of sepsis, the massive release of pro-inflammatory cytokines triggers a "cytokine storm" [21], leading to damage in vital organs such as the lungs and liver [22, 23]. Lung and liver damage significantly affects the prognosis of sepsis patients, making early diagnosis and intervention critical. Although the inflammatory mechanisms of sepsis have been explored to some extent, the regulatory pathways and targets remain incompletely understood. The aim of this study was to elucidate the role of the AGO2–ATOX1 axis in influencing the inflammatory response in sepsis, providing new targets and theoretical insights for sepsis treatment.

AGO2 is the only member of the Argonaute family with RNA cleavage activity, capable of mediating gene post-transcriptional expression through mRNA, thereby influencing cellular functions and immune responses [24]. In this study, we found that AGO2 was significantly upregulated in model mice, and specific knockdown of AGO2 effectively alleviated CLP-induced lung and liver damage, suppressed the inflammatory response, and corrected macrophage polarization imbalance. Previous studies have reported significant upregulation of AGO2 expression in the plasma during sepsis [25], and AGO2 can regulate the onset and progression of sepsis by participating in inflammatory pathways [14]. Furthermore, inhibiting AGO2 reduced iNOS levels in inflammatory mice and promoted macrophage polarization toward the M2 phenotype. AGO2-associated complexes have also been reported to act as inhibitors of iNOS protein synthesis [26]. Previous *in vitro* experiments have shown that silencing AGO2 can inhibit LPS-induced inflammatory damage, reduce M1 macrophage polarization, and promote M2 polarization. The effect of LPS on AGO2 has already been studied in peripheral macrophages [27]. Some AGO2-associated complexes have been shown to be important inflammatory regulators, with their accumulation accompanied by elevated levels of IL-6, TNF-α, and NO [28]. In our study, downregulation of AGO2 expression significantly reduced the production of inflammatory cytokines. In line with our results, downregulation of AGO2 has been shown to alleviate inflammation by reducing TNF-α and IL-1β levels in morphine-induced microglial cells via modulation of miRNA-30a-5p processing [29], and by improving the inflammatory phenotype of RAW264.7 macrophages [30]. The changes in AGO2 expression can influence the polarization state of macrophages. These findings further support the critical role of AGO2 in affecting sepsis-induced inflammatory responses and macrophage polarization.

To further explore the specific regulatory mechanism of AGO2, we found that AGO2 can bind to ATOX1 mRNA and upregulate its expression. ATOX1 is a copper chaperone protein that not only maintains cellular copper ion homeostasis and redox balance but also participates in the regulation of inflammatory signaling pathways [31]. Subsequent experiments revealed that ATOX1 was significantly upregulated in model mice, and silencing ATOX1 in RAW264.7 cells effectively alleviated the macrophage polarization imbalance and inflammatory damage induced by LPS. Previous studies have confirmed that ATOX1 can promote the production of inflammatory cytokines by influencing macrophage polarization [32]. Additionally, Kim *et al.* found that knockout of ATOX1 reduced the expression of iNOS, thereby inhibiting the MAPK and NF-κB signaling pathways and alleviating the inflammatory response [33]. Our study further demonstrated that in LPS-stimulated RAW264.7 cells, overexpression of ATOX1 reversed the anti-inflammatory effects induced by AGO2 silencing. Similarly, ATOX1 plays a critical pro-inflammatory role by promoting M1 polarization of macrophages and enhancing the production of inflammatory cytokines, while inhibition of ATOX1 leads to marked reductions in M1 polarization markers and pro-inflammatory cytokines [19]. These findings are consistent with our experimental results, further confirming that AGO2 regulates macrophage polarization through ATOX1, thereby exacerbating the inflammatory response in sepsis. Notably, this is the first study to demonstrate that AGO2 directly binds and stabilizes ATOX1 mRNA to amplify inflammatory responses in sepsis. The novelty of this regulatory axis is underscored by the RIP-qPCR results (Fig. 4), which provide direct evidence of molecular interaction. While prior research has independently implicated AGO2 or ATOX1 in immune regulation [34, 35], our work uniquely links them in a mechanistic cascade, adding a new layer to the understanding of macrophage polarization in systemic inflammation.

Although this study confirms the crucial role of the AGO2–ATOX1 axis in the inflammatory response of sepsis, certain limitations remain. The current findings are based on a septic mouse model, and due to inherent differences in the pathophysiological mechanisms between mice and humans, the clinical applicability requires further validation. For instance, mouse cytokine kinetics and immune cell subsets often differ in magnitude and timing compared to humans. Future studies should include a comparative analysis of cytokine profiles (e.g., TNF-α, IL-6, IL-1β) in CLP-induced mice vs. plasma from sepsis patients to evaluate conserved patterns. Moreover, the heterogeneity of human sepsis, affected by age, sex, genetic background, and pre-existing conditions, poses challenges to generalizing murine data. Addressing these confounding factors in future study designs will be crucial for refining translational applicability. To further bridge the translational gap, future research will focus on quantifying AGO2 and ATOX1 expression in blood samples from sepsis patients and correlating their levels with Sequential Organ Failure Assessment scores and clinical outcomes. In addition, siRNA-mediated silencing of AGO2 and ATOX1 in human monocyte-derived macrophages will be conducted to validate their roles in cytokine production and macrophage polarization. Single-cell and spatial transcriptomic datasets from human sepsis tissues will also be analyzed to confirm cell-type-specific expression patterns. Furthermore, the therapeutic potential of targeting AGO2 or ATOX1 will be evaluated using pharmacological inhibitors in humanized mouse and porcine sepsis models. Collectively, these efforts aim to determine whether modulation of the AGO2–ATOX1 axis represents a viable and effective therapeutic strategy in human sepsis.

In conclusion, this study revealed that AGO2 enhances the expression of ATOX1 by binding and stabilizing its mRNA, thereby promoting M1 macrophage polarization and inhibiting M2 polarization, which exacerbates the inflammatory response triggered by sepsis. This previously unrecognized post-transcriptional regulatory pathway offers not only mechanistic insight but also a novel target for clinical intervention. These results are expected to contribute to the further development of sepsis-related therapies and open new avenues for improving patient prognosis.

Funding

This research received no funding support from any institution or individual.

Disclosures

This study was approved by the ethics committee of the Affiliated Nanhua Hospital, Hengyang Medical School, University of South China. (Approval No.: 2025-KY-031).

The authors declare no conflict of interest.

References

1. Hawiger J, Veach RA, Zienkiewicz J (2015): New paradigms in sepsis: from prevention to protection of failing microcirculation. J Thromb Haemost 13: 1743-1756.
2. Salomão R, Ferreira BL, Salomão MC, et al. (2019): Sepsis: evolving concepts and challenges. Braz J Med Biol Res 52: e8595.
3. Nedeva C (2021): Inflammation and cell death of the innate and adaptive immune system during sepsis. Biomolecules 11: 1011.
4. De Freitas Caires N, Gaudet A, Portier L, et al. (2018): Endocan, sepsis, pneumonia, and acute respiratory distress syndrome. Crit Care 22: 280.
5. Gotts JE, Matthay MA (2016): Sepsis: pathophysiology and clinical management. BMJ 353: i1585.
6. Rudd KE, Johnson SC, Agesa KM, et al. (2020): Global, regional, and national sepsis incidence and mortality, 1990-2017: analysis for the Global Burden of Disease Study. Lancet 395: 200-211.
7. Fowler AA, 3rd, Truwit JD, Hite RD, et al. (2019): Effect of vitamin C infusion on organ failure and biomarkers of inflammation and vascular injury in patients with sepsis and severe acute respiratory failure: The CITRIS-ALI Randomized Clinical Trial. JAMA 322: 1261-1270.
8. Yunna C, Mengru H, Lei W, et al. (2020): Macrophage M1/M2 polarization. Eur J Pharmacol 877: 173090.
9. Butt Y, Kurdowska A, Allen TC (2016): Acute lung injury: A clinical and molecular review. Arch Pathol Lab Med 140: 345-350.
10. Chen X, Liu Y, Gao Y, et al. (2021): The roles of macrophage polarization in the host immune response to sepsis. Int Immunopharmacol 96: 107791.
11. Lobo V, Nowak I, Fernandez C, et al. (2024): Loss of Lamin A leads to the nuclear translocation of AGO2 and compromised RNA interference. Nucleic Acids Res 52: 9917-9935.
12. Lessel D, Zeitler DM, Reijnders MRF, et al. (2020): Germline AGO2 mutations impair RNA interference and human neurological development. Nat Commun 11: 5797.
13. Machado-Pereira M, Saraiva C, Bernardino L, et al. (2022): Argonaute-2 protects the neurovascular unit from damage caused by systemic inflammation. J Neuroinflammation 19: 11.
14. Zou Z, Lin Q, Yang H, et al. (2020): Nrp-1 mediated plasmatic Ago2 binding miR-21a-3p internalization: A novel mechanism for miR-21a-3p accumulation in renal tubular epithelial cells during sepsis. Biomed Res Int 2020: 2370253.
15. Bam M, Yang X, Zumbrun EE, et al. (2017): Decreased AGO2 and DCR1 in PBMCs from War Veterans with PTSD leads to diminished miRNA resulting in elevated inflammation. Transl Psychiatry 7: e1222.
16. Maung MT, Carlson A, Olea-Flores M, et al. (2021): The molecular and cellular basis of copper dysregulation and its relationship with human pathologies. FASEB J 35: e21810.
17. Das A, Sudhahar V, Ushio-Fukai M, et al. (2019): Novel interaction of antioxidant-1 with TRAF4: role in inflammatory responses in endothelial cells. Am J Physiol Cell Physiol 317: C1161-C1171.
18. Xu D, Zhu W, Ding C, et al. (2023): Self-homeostasis immunoregulatory strategy for implant-related infections through remodeling redox balance. ACS Nano 17: 4574-4590.
19. Chen M, Chen Y, Fu R, et al. (2024): Atox1 regulates macrophage polarization in intestinal inflammation via ROS-NLRP3 inflammasome pathway. J Transl Med 22: 497.
20. Li C, Yu L, Mai C, et al. (2021): KLF4 down-regulation resulting from TLR4 promotion of ERK1/2 phosphorylation underpins inflammatory response in sepsis. J Cell Mol Med 25: 2013-2024.
21. Delano MJ, Ward PA (2016): The immune system's role in sepsis progression, resolution, and long-term outcome. Immunol Rev 274: 330-353.
22. Ma S, Evans R G, Iguchi N, et al. (2019): Sepsis-induced acute kidney injury: A disease of the microcirculation. Microcirculation 26: e12483.
23. Ehlting C, Wolf SD, Bode JG (2021): Acute-phase protein synthesis: a key feature of innate immune functions of the liver. Biol Chem 402: 1129-1145.
24. Zhang K, Pomyen Y, Barry AE, et al. (2020): AGO2 mediates MYC mRNA stability in hepatocellular carcinoma. Mol Cancer Res 18: 612-622.
25. Arroyo JD, Chevillet JR, Kroh EM, et al. (2011): Argonaute2 complexes carry a population of circulating microRNAs independent of vesicles in human plasma. Proc Natl Acad Sci U S A 108: 5003-5008.
26. Guo Z, Geller DA (2014): microRNA and human inducible nitric oxide synthase. Vitam Horm 96: 19-27.
27. Mazumder A, Bose M, Chakraborty A, et al. (2013): A transient reversal of miRNA-mediated repression controls macrophage activation. EMBO Rep 14: 1008-1016.
28. De Kerckhove M, Tanaka K, Umehara T, et al. (2018): Targeting miR-223 in neutrophils enhances the clearance of Staphylococcus aureus in infected wounds. EMBO Mol Med 10: e9024.
29. Wan L, Jia RM, Ji LL, et al. (2022): AMPK-autophagy-mediated inhibition of microRNA-30a-5p alleviates morphine tolerance via SOCS3-dependent neuroinflammation suppression. J Neuroinflammation 19: 25.
30. Yu H, Qin L, Peng Y, et al. (2020): Exosomes derived from hypertrophic cardiomyocytes induce inflammation in macrophages via miR-155 mediated MAPK pathway. Front Immunol 11: 606045.
31. Sudhahar V, Shi Y, Kaplan JH, et al. (2022): Whole-transcriptome sequencing analyses of nuclear antixoxidant-1 in endothelial cells: role in inflammation and atherosclerosis. Cells 11: 2919.
32. Zou M, Zhang W, Zhu Y, et al. (2023): Identification of 6 cuproptosis-related genes for active ulcerative colitis with both diagnostic and therapeutic values. Medicine (Baltimore) 102: e35503.
33. Kim DW, Shin MJ, Choi YJ, et al. (2018): Tat-ATOX1 inhibits inflammatory responses via regulation of MAPK and NF-κB pathways. BMB Rep 51: 654-659.
34. Wang Y, Chen Z, Liang K, et al. (2025): AGO2 mediates immunotherapy failure via suppressing tumor IFN-gamma response-dependent CD8(+) T cell immunity. Cell Rep 44: 115445.
35. Yu H, Si G, Si F (2024): Mendelian randomization validates the immune landscape mediated by aggrephagy in esophageal squamous cell carcinoma patients from the perspectives of multi-omics. J Cancer 15: 1940-1953.